2021

Multifractional Brownian Motion and Its Applications to Factor Analysis on Consumer Confidence Index

Christopher Box

Claremont McKenna College

Multifractional Brownian Motion and Its Applications to Factor Analysis on Consumer Confidence Index

submitted to
Qidi Peng (Mathematical Sciences, Claremont Graduate University)
Asuman G. Aksoy (Mathematical Sciences, Claremont McKenna College)
Yunied Puig de Dios (Mathematical Sciences, Claremont McKenna College)

by
Christopher Joseph Box

for
Senior Thesis
8th Semester, 2021
April 27, 2021

Contents

1 Introduction **3**

2 A Review on Brownian Motion **4**
2.1 Introduction and Definition of Brownian Motion 4

3 Properties of Brownian Motion **5**
3.1 Normality of Brownian Motion 5
3.2 Covariance Structure of Brownian Motion 5
3.3 Self Similarity of Brownian Motion 7
3.4 Representations of Brownian Motion 9
3.5 Sample Paths Properties of Brownian Motion 10

4 Introduction to Fractional Brownian Motion **10**
4.1 Definition of Fractional Brownian Motion 10
4.2 Some Key Properties of Fractional Brownian Motion 12

5 From Fractional Brownian Motion to Multifractional Brownian Motion **15**
5.1 A General Class of Multifractional Processes 16
5.2 LGQV Estimation of the Pointwise Hölder Exponent 17

6 Real World Application: Factor Analysis on Consumer Confidence Index **20**

7 Model Specifics: Limitations and Future Applications **24**

Acknowledgements

First, I want to thank **Professor Qidi Peng** from Claremont Graduate University for his oversight and help with this thesis. His oversight and guidance were critical to the completion of my work. On his research team, I want to thank **Yujia Ding** for her help with coding in Matlab and Python, and **Chengcheng Zhang** for her help with providing economics background of the application section. I acknowledge **Professors Asuman G. Aksoy** and **Yunied Puig de Dios** for reviewing my thesis manuscript, attending my oral presentation and providing valuable feedback, which improved the last version of the manuscript. I also want to thank my other professors for previously preparing me to undertake this project: **Professors Sam Nelson**, **Chiu-Yen Kao**, **Michael Orrison**, **Mark Huber**, and **Henry Schellhorn**.

I would thank my friends, housemates, and siblings: Kevin Box, Caroline Box, Emily Warner, Rob Driscol, Sean Pine, Nic Hernandez, Christian Thornton, Patrick Tandy, Zack Rossman, Ethan Lewis, Harrison Miller, Garegin Soghomonyan, Amadeo Cantu-Trevino, Noah Smith, Andrew Wraith, Will Clark, Sam Harrison, Eric Warmoth, Kyle Ballack, Ben Weldon, Noah Weldon, Nick Maramica, and the Freshmen.

Most importantly a special thanks to my parents, **Michelle Box** and **Mark Box** for always supporting me, especially at the presentation.

Abstract

This thesis aims at introducing a new way to model time series objects in statistics using multifractional processes. It provides a detailed review of Brownian motion, fractional Brownian motion and extends the above 2 models to multifractional processes. To demonstrate a successful application to the real world, we perform pattern analysis on consumer confidence and household spending behavior. The analysis is conducted through investigating the local Hölder regularity of the consumer confidence index and household expenditure. In the analysis, we first model consumer confidence index and household expenditure with a multifractional stochastic processes. We then use the index, pointwise Hölder exponent (PHE), to measure the local Hölder regularity of their paths. Next several estimators of the PHE have been derived and compared using the data. Finally, we detect which household consumption factors share similar patterns of local Hölder regularity to the CCI using K-means clustering.
Keywords: consumer confidence index; household spending behavior; multifractional process; pointwise Hölder exponent; nonparametric estimation; Brownian motion

1 Introduction

Multifractional Brownian motion (mBm) is a paradigmatic example of both multifractional stochastic processes and locally asymptotically self-similar processes. It naturally extends the classical fractional Brownian motion (fBm) by allowing its Hurst parameter to vary with time. The mBm was introduced independently by Peltier and Lévy-Véhel [21] and Benassi et al. [6], using respectively integral moving average type representation and harmonizable integral representation of the fBm. These two types of mBms share a number of core features and their precise connection has been studied by Stoev and Taqqu [28], who show that the two types of mBms generally have different correlation structures. The most recent discussion on the definition of mBm is also made in [28], where they define a general class of multifractional Gaussian processes which includes the above two types of mBms as 2 particular cases. In this thesis we adopt the definition of an mBm through the so-called harmonizable integral representation (see (1.3) in [28] or see [6, 1]).

Definition 1.1 *A multifractional Brownian motion $\{X(t)\}_{t\geq 0}$ is a continuous-time Gaussian process defined by:*

$$X(0) = 0 \text{ a.s. and } X(t) = \int_{\mathbb{R}} \frac{e^{it\xi} - 1}{|\xi|^{H(t)+1/2}} \, \mathrm{d}\widetilde{W}(\xi), \text{ for } t > 0, \tag{1.1}$$

where:

- $\mathrm{d}\widetilde{W}(\xi)$ *denotes a complex-valued Gaussian measure (see Proposition 2.1 in [28]) satisfying*

$$\int_{\mathbb{R}} \widetilde{f}(\xi) \, \mathrm{d}\widetilde{W}(\xi) = \int_{\mathbb{R}} f(t) \, \mathrm{d}W(t) \text{ a.s.}$$

  for any

$$f \in L^2(\mathbb{R}) := \left\{ \{ f : \mathbb{R} \to \mathbb{R} \} : \int_{\mathbb{R}} |f(u)|^2 \, \mathrm{d}u < \infty \right\}, \tag{1.2}$$

  with $\widetilde{f}(\xi) := (2\pi)^{-1/2} \int_{\mathbb{R}} e^{i\xi u} f(u) \, \mathrm{d}u$ being the Fourier transform of f and $\{W(t)\}_{t\in\mathbb{R}}$ being a standard Brownian motion.

- *The functional Hurst parameter $H : [0, +\infty) \longrightarrow (0, 1)$ is a Hölder function with exponent $\beta > \sup_{t\in[0,+\infty)} H(t)$. It is known that the pointwise Hölder exponent (pHe) of $\{X(t)\}_{t\geq 0}$ is almost surely equal to $H(\bullet)$ at each t [6]. Recall that, for a continuous nowhere differentiable process $\{Y(t)\}_{t\geq 0}$, its local Hölder regularity can be measured by the pHe ρ_Y defined by: for each $t_0 \geq 0$,*

$$\rho_Y(t_0) := \sup \left\{ \alpha \in [0, 1] : \limsup_{\varepsilon \to 0} \frac{|Y(t_0 + \epsilon) - Y(t_0)|}{|\varepsilon|^\alpha} = 0 \right\}.$$

Theorem 4.1 in [28] gives the covariance function of $\{X(t)\}_{t\geq 0}$: for $s,t\geq 0$,

$$\mathbb{C}ov(X(s),X(t))=\frac{K(H(s)+H(t))}{2}\left(|s|^{H(s)+H(t)}+|t|^{H(s)+H(t)}-|s-t|^{H(s)+H(t)}\right), \tag{1.3}$$

where the scaling parameter $K(\bullet)$ is defined by

$$K(\alpha):=\frac{4\cos(\alpha\pi/2)\Gamma(2-\alpha)}{\alpha(1-\alpha)},\quad \text{for } \alpha\in(0,2), \tag{1.4}$$

with $\Gamma(\bullet)$ being the gamma function. When $\alpha=1$ (corresponding to $H(\bullet)\equiv 1/2$), the value of $\cos(\alpha\pi/2)/(1-\alpha)$ is set to be $\pi/2$ (indeed, $\cos(\alpha\pi/2)/(1-\alpha)\to\pi/2$ as $\alpha\to 1$). As a consequence, $K(1)=1$. Hence mBm includes standard Brownian motion as one special case: $H(\bullet)\equiv 1/2$.

From a number of perspectives, mBm naturally extends fBm. MBm becomes an fBm when its pHe is almost surely equal to a constant. It is also known that mBm is locally asymptotically self-similar and its tangent process is an fBm [6, 13]. Many statistical inference problems concerning the mBm given in Definition 1.1 have been studied. For example, estimation of the pHe of multifractional processes driven by an mBm has been studied in [15, 3, 24, 25, 17, 26]. Applications of mBm in modeling currency exchange rates, market stock indices and individual stock prices are also proved to be successful [12, 10, 27, 26].

The goal of my thesis is to provide a detailed review of the literature from Brownian motion (also called Wiener process in the theory of stochastic process) to multifractional Brownian motion. The review includes concepts, properties and estimation methodologies of the above stochastic processes. Moreover, an application of the multifractional processes modeling is successfully performed. By using the multifractional process modeling, we are able to perform a new type of factor analysis on the Consumer Confidence Index. As a conclusion, the important factors are found to heavily explain the volatility of the Consumer Confidence Index.

2 A Review on Brownian Motion

This section is devoted to reviewing the benchmark stochastic process Brownian motion in the existing literature. The proofs are given for some key features of the Brownian motion.

2.1 Introduction and Definition of Brownian Motion

Brownian motion, as a physics phenomena, is originally introduced to describe the movement of a single particle suspended in a liquid. Later it was proved that this movement for one particle moving in a one-dimensional line can be modeled by a continuous- time Gaussian stochastic process. The mathematical model was introduced by Mandelbrot and Van Ness in 1968 [19] and applied across biology, hydrology, and the stock market since.

Brownian motion is named based on historical connection with the physical process of the same name originally observed by Scottish botanist Robert Brown. In mathematics, especially stochastic process analysis, it is also called Wiener process in honor of the American mathematician Norbert Wiener for his investigations on the mathematical properties of the one-dimensional Brownian motion [33]. Brownian motion is one of the best known Lévy processes (stochastic processes with stationary and independent increments) and occurs frequently in pure and applied mathematics, economics, quantitative finance, evolutionary biology, and physics.

Brownian motion plays an important role in both pure and applied mathematics. In pure mathematics, Brownian motion gave rise to the study of continuous time martingales. It is a key process in terms of which more complicated stochastic processes can be described. As such, it plays a vital role in stochastic calculus, diffusion processes and even potential theory. It is the driving process of Schramm–Loèwner evolution. In applied mathematics, the Wiener process is used to represent the integral of a white noise Gaussian process, and so is useful as a model of noise in electronics engineering, instrument errors in filtering theory and disturbances in control theory.

Below we provide the mathematical definition of Brownian motion.

Definition 2.1 *The Brownian motion $\{W_t\}_{t\geq 0}$ is a continuous-time centered Gaussian process such that*

(i) $W_0 = 0$ *almost surely.*

(ii) *The increments of $\{W_t\}_{t\geq 0}$ are independent: for any $0 \leq t_1 \leq t_2 \leq \ldots \leq t_n$, the increments*

$$W(t_2) - W(t_1), W(t_3) - W(t_2), \ldots, W(t_n) - W(t_{n-1})$$

are independent.

(iii) *The increments of $\{W_t\}_{t\geq 0}$ are stationary and normal: for any $t \geq 0$, any $h > 0$, the increments*

$$W(t+h) - W(t) \sim \mathcal{N}(0, h),$$

where $\mathcal{N}(0, h)$ denotes the Gaussian probability distribution with mean 0 and variance h.

3 Properties of Brownian Motion

Based on Definition 2.1, a number of nice features can be derived. Below we list some key properties and provide necessary proofs. From the proofs we see they are just straightforward consequences of the L 'evy properties: stationary independent increments.

3.1 Normality of Brownian Motion

Brownian motion is a Gaussian Process. Each point of the process follows the unconditional probability density function, which follows normal distribution with zero-mean and variance t, at a fixed time t:

$$f_{W_t}(x) = \frac{1}{\sqrt{2\pi t}} e^{-x^2/(2t)}.$$

The expectation is zero:

$$\mathbb{E}[W_t] = 0.$$

The variance, using the computational formula, is t:

$$\mathbb{V}ar(W_t) = t.$$

These results follow immediately from the definition that increments have a normal distribution, centered at zero. Thus:

$$W_t = W_t - W_0 \sim \mathcal{N}(0, t).$$

3.2 Covariance Structure of Brownian Motion

We look to measure the dependency between points within the Brownian Motion by calculating the covariance and correlation of increments.

Proposition 3.1 *The covariance and correlation of the Bm $\{W_t\}_{t\geq 0}$ are given as: for any $s, t > 0$,*

$$\mathbb{C}ov(W_s, W_t) = \min\{s, t\} \tag{3.1}$$

and

$$\mathbb{C}orr(W_s, W_t) = \sqrt{\frac{\min\{s,t\}}{\max\{s,t\}}}. \tag{3.2}$$

Proof: Without loss of generality, let $0 < t_1 \leq t_2$. We first prove (3.1) holds. By the definition of the covariance function and the fact that the Bm $\{W_t\}_{t\geq 0}$ is zero-mean, we have

$$\mathbb{C}ov(W_{t_1}, W_{t_2}) = \mathbb{E}\left[W_{t_1} W_{t_2}\right]. \tag{3.3}$$

By (3.3) we decompose W_{t_2} into the sum of increments:

$$W_{t_2} = (W_{t_2} - W_{t_1}) + W_{t_1}. \tag{3.4}$$

It follows from (3.3), (3.4) and the fact that expectation is a linear operator that

$$\begin{aligned} \mathbb{C}ov(W_{t_1}, W_{t_2}) &= \mathbb{E}\left[W_{t_1}((W_{t_2} - W_{t_1}) + W_{t_1})\right] \\ &= \mathbb{E}\left[W_{t_1}(W_{t_2} - W_{t_1})\right] + \mathbb{E}\left[W_{t_1}^2\right]. \end{aligned} \tag{3.5}$$

On one hand, by Definition 2.1 **(ii)**, $W_{t_1} = W_{t_1} - W_{t_0}$ and $W_{t_2} - W_{t_1}$ are independent; and by Definition 2.1 **(iii)**, $\mathbb{E}[W_{t_2} - W_{t_1}] = 0$. As a result,

$$\mathbb{E}\left[W_{t_1}(W_{t_2} - W_{t_1})\right] = \mathbb{E}[W_{t_1}]\mathbb{E}[W_{t_2} - W_{t_1}] = 0. \tag{3.6}$$

On the other hand, by Definition 2.1 **(iii)**,

$$\mathbb{E}\left[W_{t_1}^2\right] = \mathbb{V}ar(W_{t_1}) = t_1. \tag{3.7}$$

Finally plugging (3.6) and (3.7) into 3.5, we obtain

$$\mathbb{C}ov(W_{t_1}, W_{t_2}) = 0 + \mathbb{E}\left[W_{t_1}^2\right] = t_1.$$

(3.1) is proved.

Next we prove (3.2). Again assume $0 < t_1 \leq t_2$ without loss of generality. On one hand, by the definition of correlation coefficient, we can write

$$\mathbb{C}orr(W_{t_1}, W_{t_2}) = \frac{\mathbb{C}ov(W_{t_1}, W_{t_2})}{\sqrt{\mathbb{V}ar(W_{t_1})\mathbb{V}ar(W_{t_2})}}.$$

On the other hand by using (3.1) we have

$$\mathbb{C}ov(W_{t_1}, W_{t_2}) = t_1;\ \mathbb{V}ar(W_{t_1}) = t_1 \text{ and } \mathbb{V}ar(W_{t_2}) = t_2.$$

Plugging the above equations into the expression of $Corr(W_{t_1}, W_{t_2})$ finally yields

$$\mathbb{C}orr(W_{t_1}, W_{t_2}) = \frac{t_1}{\sqrt{t_1 t_2}} = \sqrt{\frac{t_1}{t_2}}.$$

(3.2) holds true hence the proof of Proposition 3.1 is complete. □ Note that in the proof of Proposition 3.1, all the features of Bm in Definition 2.1 are involved. In fact, Proposition 3.1 is an equivlaent definition of Bm. To be more specific, a Bm can be defined as follows:

Definition 3.2 *The Brownian motion $\{W_t\}_{t\geq 0}$ is defined to be a continuous-time centered Gaussian process with*

$$W_0 = 0 \text{ almost surely and } \mathbb{C}ov(W_s, W_t) = \min\{s, t\}, \text{ for any } s, t > 0.$$

Proposition 3.1 below establishes the equivalence between Definition 2.1 and Definition 3.2.

Proposition 3.3 *By Definition 3.2, the Brownian motion $\{W_t\}_{t\geq 0}$ has independent and stationary increments.*

Proof: Let $0 < t_1 \leq t_2$. By Definition 3.2 we know

$$\mathbb{C}ov(W_{t_1}, W_{t_2}) = t_1. \tag{3.8}$$

Take W_{t_1} and $W_{t_2} - W_{t_1}$ as 2 increments of the Bm. Remark that the independence of stationarity of the increments can be interpreted as

(i) $\mathbb{C}ov(W_{t_1}, W_{t_2} - W_{t_1}) = 0$;

(ii) $W_{t_2} - W_{t_1} \sim \mathcal{N}(0, t_2 - t_1)$.

To show **(i)** holds we rely on (3.8):

$$\mathbb{C}ov(W_{t_1}, W_{t_2} - W_{t_1}) = \mathbb{C}ov(W_{t_1}, W_{t_2}) - \mathbb{C}ov(W_{t_1}, W_{t_1}) = \min\{t_1, t_2\} - t_1 = 0.$$

It remains to show **(ii)** holds. First since Bm is a Gaussian process, $W_{t_2} - W_{t_1}$ is then normally distributed. It suffices to determine the mean and variance of $W_{t_2} - W_{t_1}$ to get its exact probability distribution. On one hand, by the fact that Bm is centered,

$$\mathbb{E}[W_{t_2} - W_{t_1}] = \mathbb{E}[W_{t_2}] - \mathbb{E}[W_{t_1}] = 0 - 0 = 0. \tag{3.9}$$

On the other hand, we use the definition of variance and the covariance function of Bm to obtain

$$\begin{aligned} \mathbb{V}ar(W_{t_2} - W_{t_1}) &= \mathbb{V}ar(W_{t_2}) + \mathbb{V}ar(W_{t_1}) + 2\mathbb{C}ov(W_{t_2}, -W_{t_1}) \\ &= t_2 + t_1 - 2t_1 = t_2 - t_1. \end{aligned} \tag{3.10}$$

It follows from (3.9) and (3.10) that **(ii)** holds true. The prof is complete. □ Let us explain why **(ii)** is equivalent to stationary increments. Remark that by **(ii)**, should we shift the increment by $h \geq 0$, we obtain

$$\mathbb{V}ar(W_{t_2+h} - W_{t_1+h}) = (t_2 + h) - (t_1 + h) = t_2 - t_1.$$

We can see that the shift does not change the probability distribution as the mean and variance are not dependent on W_t, hence the increments are stationary. Therefore we have confirmed that the increments of Bm are stationary.

3.3 Self Similarity of Brownian Motion

The self-similarity of Borwnian motion is described in the following statement.

Proposition 3.4 *Let $\{W_t\}_{t\geq 0}$ be a Brownian motion. For every $c > 0$ the process $V_t = (1/\sqrt{c})W_{ct}$ is another Brownian motion.*

Proof: Fix $c > 0$. Since $\{W_t\}_{t\geq 0}$ is a Gaussian process, so is $\{V_t\}_{t\geq 0} = \{(1/\sqrt{c})W_{ct}\}_{t\geq 0}$ since it a linear combination of a Gaussian Process. Then it suffices to show that V_t satisfies Definition 3.2 of Brownian motion.

1. Show $V_0 = 0$ almost surely. By the definition of V_t and the fact that $W_0 = 0$ almost surely, we have
$$V_0 = (1/\sqrt{c})W_{c\times 0} = (1/\sqrt{c})W_0 = (1/\sqrt{c}) \times 0 = 0, \text{ almost surely.} \tag{3.11}$$
2. Show $\mathbb{E}[V_t] = 0$ for all $t \geq 0$. This is obviously true
$$\mathbb{E}[V_t] = \mathbb{E}[(1/\sqrt{c})W_{ct}] = (1/\sqrt{c})\mathbb{E}[W_{ct}] = 0. \tag{3.12}$$

3. Show the covariance of the increments of $\{V_t\}_{t\geq 0}$ satisfies Equation 3.1.

   Let $0 < s < t$, then by definition of V_t we can write

$$V_s = (1/\sqrt{c})W_{cs} \text{ and } V_t = (1/\sqrt{c})W_{ct}. \tag{3.13}$$

   Below we would show $\mathbb{C}ov(V_s, V_t) = s$. Using (3.13) we compute $\mathbb{C}ov(V_s, V_t)$ as

$$\mathbb{C}ov(V_s, V_t) \quad = \quad \mathbb{C}ov\left(\frac{W_{cs}}{\sqrt{c}}, \frac{W_{ct}}{\sqrt{c}}\right) = \frac{\mathbb{C}ov(W_{cs}, W_{ct})}{c}. \tag{3.14}$$

   Recall that $\mathbb{C}ov(W_s, W_t) = s$ for any $0 \leq s \leq t$. Since $c > 0$ we have $cs < ct$, it yields $\mathbb{C}ov(W_{cs}, W_{ct}) = cs$. Plugging this result into (3.14) obtains

$$\mathbb{C}ov(V_s, V_t) = \frac{cs}{c} = s. \tag{3.15}$$

From Equations (3.11) - (3.15), we see $\{V_t\}_{t\geq 0}$ is a Brownian motion, based on Definition 3.2 □

The next feature is particularly owned by Bm. It shows that the Bm is preserved through time reversal.

Proposition 3.5 *The process* $\{V_t\}_{t\in[0,1]} = \{W_1 - W_{1-t}\}_{t\in[0,1]}$ *is distributed like* $\{W_t\}_{t\in[0,1]}$.

Proof: Obviously $\{V_t\}_{t\geq 0}$ is a Gaussian process. Next we show $V_0 = 0$ a.s., $\mathbb{E}[V_t] = 0$ and $\mathbb{C}ov(V_s, V_t) = s$ for $0 \leq s \leq t \leq 1$.

1. Show $V_0 = 0$ a.s.. By definition of V_t:

$$V_0 = W_1 - W_{1-0} = W_1 - W_1 = 0, \text{ a.s..} \tag{3.16}$$

2. Show $\mathbb{E}[V_t] = 0$. Using the definition of V_t and linearity of expectation:

$$\mathbb{E}[V(t)] = \mathbb{E}[W_1 - W_{1-t}] = \mathbb{E}[W_1] - \mathbb{E}[W_{1-t}] = 0 - 0 = 0. \tag{3.17}$$

3. Show the covariance structure of $\{V_t\}_{t\in[0,1]}$ follows Equation 3.1 for $0 \leq s \leq t \leq 1$.

   Recall that the covariance function is bilinear: for any 4 random variables X_1, X_2, X_3, X_4:

$$\mathbb{C}ov(X_1 + X_2, X_3 + X_4) = \sum_{i\in\{1,2\}, j\in\{3,4\}} \mathbb{C}ov(X_i, X_j).$$

   Therefore together with the Bm's covariance structure we can write

$$\begin{aligned}
&\mathbb{C}ov(V_s, V_t) = \mathbb{C}ov(W_1 - W_{1-s}, W_1 - W_{1-t}) \\
&= \mathbb{C}ov(W_1, W_1) - \mathbb{C}ov(W_1, W_{1-t}) - \mathbb{C}ov(W_{1-s}, W_1) + \mathbb{C}ov(W_{1-s}, W_{1-t}) \\
&= 1 - \min\{1, 1-t\} - \min\{1-s, 1\} + \min\{1-s, 1-t\} \\
&= 1 - (1-t) - (1-s) + (1-t) \\
&= s.
\end{aligned} \tag{3.18}$$

From equations (3.16) - (3.18), $\{V_t\}_{t\geq 0}$ is a Brownian Motion, based on Definition 3.2. □

The following property shows Bm can be preserved through time inversion.

Proposition 3.6 *The process* $\{V_t\}_{t\geq 0} = \{tW_{1/t}\}_{t\geq 0}$ *is a Brownian motion.*

Proof: Similar to the proofs of the above propositions, first of all it is easy to derive that $\{V_t\}_{t\geq 0}$ is a centered Gaussian process. It then suffices to show $V_0 = 0$ a.s. and $\mathbb{C}ov(V_s, V_t) = s$ for $0 \leq s \leq t$.

1. Show $V_0 = 0$ almost surely. Recall that

$$V_t = tW_{1/t} \sim \mathcal{N}(0, t).$$

This yields when $t \to 0$, $\mathbb{V}ar(V_t) \to 0$. Therefore V_0 is almost surely a constant. Observe that $\mathbb{E}[V_0] = 0$, then

$$V_0 = 0 \text{ a.s..} \tag{3.19}$$

2. Show the covariance of the increments of $\{V_t\}_{t\geq 0}$ follows Definition 3.2.

Let $0 \leq s \leq t$, then $V_s = sW_{1/s}$ and $V_t = tW_{1/t}$. Using these expression we get

$$\begin{aligned} &\mathbb{C}ov(V_s, V_t) = \mathbb{C}ov(sW_{1/s}, tW_{1/t}) = st \times \mathbb{C}ov(W_{1/s}, W_{1/t}) \\ &= st \times \min(1/s, 1/t) = st \times \frac{1}{t} = s. \end{aligned} \tag{3.20}$$

From Equations (3.19) and (3.20), $\{V_t\}_{t\geq 0}$ is a Brownian motion.

□

3.4 Representations of Brownian Motion

Representations of Bm have been heavily studied, since these properties are needed in order to better understand the link between Bm and white noises. Another reason is representations allow one to simulate the Bm's paths. So far in the literature, there exist two main types of representations of Brownian motions. One is based on the moving average representation from white noise, the other one is based on Fourier transformation of the Brownian measure. The first presentation is widely used to simulate the Brownian motion process, while the second one is often used to extend Brownian motion to a more sophisticated processes such as fractional Brownian motion and multifractional Brownian motion (see the forthcoming sections).

The first representation of Brownian motion given by Wiener [33] gave a representation of a Brownian path in terms of a random Fourier series. Already very well known, this is the white noise, Gaussian noise representation, or the moving average representation. If ξ_n's are independent Gaussian variables with mean 0 and variance 1, then (see [33]):

$$W_t = \xi_0 t + \sqrt{2}\sum_{n=1}^{\infty} \xi_n \frac{\sin \pi n t}{\pi n}.$$

Here the first term represents the trend and the second term the noise for the function as grows, hence the moving average naming.

The other representation is called the harmonizable integral representation of Brownian Motion. From now on we will rely more on this representation to describe Brownian motions, as it is a much better fit for our application. The integral is obtained using through a complex-valued Fourier transformation of some deterministic signal.

$$W_t = \int_{-\infty}^{+\infty} \frac{e^{it\xi} - 1}{|\xi|} \, \mathrm{d}\widetilde{W}(\xi),$$

where $\widetilde{W}(\xi)$ denotes the Fourier transformation of a Brownian measure $W(\xi)$ (see (1.2) for the definition of Fourier transformation of a Brownian measure). The above integral representation defines the standard Brownian motion. As a representation it is more elegant than convergent series and it provides a much easier computation formula of the variance for our analysis. The covariance function of Bm is hence viewed as an inner product structure of the $L^2(\mathbb{P})$ space:

$$\mathbb{C}ov(W_s, W_t) = \int_{\mathbb{R}} \frac{(e^{it\xi} - 1)(e^{-is\xi} - 1)}{|\xi|^2} \, \mathrm{d}\xi.$$

In particular, another integral representation of the variance function of Bm is obtained:

$$\mathbb{V}ar(W_t) = \mathbb{C}ov(W_t, W_t) = \int_{\mathbb{R}} \frac{|e^{it\xi} - 1|^2}{|\xi|^2} \, \mathrm{d}\xi.$$

3.5 Sample Paths Properties of Brownian Motion

The improvements of Brownian motion are inspired by their roughness of sample paths. Concerning the sample paths properties of a Brownian motion, the key feature is that the paths of a Bm is continuous but nowhere differentiable functions. These features are captured by the so-called law of the iterated logarithm of Bm:

- Law of the iterated logarithm:

$$\limsup_{t \to +\infty} \frac{|W_t|}{\sqrt{2t \log\log t}} = 1, \quad \text{almost surely.}$$

- Modulus of continuity:

$$\limsup_{\varepsilon \to 0+} \frac{|W_\varepsilon|}{\sqrt{2\varepsilon \log\log(1/\varepsilon)}} = 1, \qquad \text{almost surely.}$$

- Lévy's global modulus of continuity:

$$\limsup_{\varepsilon \to 0+} \sup_{0 \le s < t \le 1, t-s \le \varepsilon} \frac{|W_s - W_t|}{\sqrt{2\varepsilon \log(1/\varepsilon)}} = 1, \qquad \text{almost surely.}$$

All the above sample paths properties suggest

$$|W_t - W_s| \approx |t - s|^{1/2-\varepsilon} \text{ for } |t-s| \text{ small and } \varepsilon \text{ arbitrarily small.}$$

This indicates that $1/2$ is a key parameter to capture the sample paths behavior of Bm. It is infact the Hölder exponent of Brownian motion. In other words, all Brownian motion's paths are almost surely Hölderian functions with Hölder exponent $1/2$. This accurately explains why Bm's sample paths are continuous but nowhere differentiable. Inspired by this fact, it is naturally to extend this parameter to arbitrary $H \in (0,1)$, in order to obtain a more general family of Gaussian processes. The latter family is the so-called fractional Brownian motion, which is discussed in the next section.

4 Introduction to Fractional Brownian Motion

We can expand the Brownian motion into the a fractional Brownian motion by introducing a sample paths parameter, the so-called Hurst exponent.

4.1 Definition of Fractional Brownian Motion

Fractional Brownian motion (fBm) is a natural generalization of Brownian motion. Unlike classical Brownian motion, the increments of fBm need not be independent.

Definition 4.1 *Fractional Brownian motion is a continuous-time Gaussian process $B_H(t)$ on $t \ge 0$, that starts at 0, has expectation 0 for all t, and has the following covariance function: for any $s, t \ge 0$,*

$$\mathbb{C}ov(B_H(s), B_H(t)) = \frac{1}{2}(|t|^{2H} + |s|^{2H} - |t-s|^{2H}), \tag{4.1}$$

where H is a real number in $(0,1)$, called the Hurst index or Hurst parameter associated with the fractional Brownian motion.

The Hurst exponent describes the raggedness of the resultant motion, with a higher value leading to a smoother motion. It was introduced by Mandelbrot and van Ness (1968). For $H = 1/2$, the covariance function of fBm becomes

$$\mathbb{C}ov(B_H(s), B_H(t)) = \frac{1}{2}(|t|+|s|-|t-s|) = \min(s,t), \tag{4.2}$$

which makes it the same as Brownian motion.

The value of H determines what kind of process the fBm is by characterizing the correlation of the increments. We begin by determining the correlation function of the increments of fBm. Let $B_H(t)$ and $B_H(t+h)$ be two points of fractional Brownian motion. The correlation of the increment $B_H(t+h) - B_H(t)$ is defined as

$$\mathbb{C}orr(B_H(t), B_H(t+h) - B_H(t)) = \frac{\mathbb{C}ov\left(B_H(t), B_H(t+h)) - B_H(t)\right)}{\sqrt{\mathbb{V}ar(B_H(t))\mathbb{V}ar(B_H(t+h) - B_H(t))}}. \tag{4.3}$$

Now from the forthcoming Proposition 4.5, we know that fBm has stationary increments, i.e., $B_H(t+h) - B_H(t) \sim B_H((t+h)-t) = B_H(h)$, which yields that Equation (4.3) becomes:

$$\mathbb{C}orr(B_H(t), B_H(t+h) - B_H(t)) = \frac{\mathbb{C}ov\left(B_H(t), B_H(t+h) - B_H(t)\right)}{\sqrt{\mathbb{V}ar(B_H(t))\mathbb{V}ar(B_H(h))}}. \tag{4.4}$$

Further using the linearity of the covariance function and (4.1), Equation () can be written as

$$\begin{aligned}
&\mathbb{C}orr(B_H(t), B_H(t+h) - B_H(t)) \\
&= \frac{\mathbb{C}ov\left(B_H(t), B_H(t+h)\right) - \mathbb{C}ov\left(B_H(t), B_H(t)\right)}{\sqrt{\mathbb{V}ar(B_H(t))\mathbb{V}ar(B_H(h))}} \\
&= \frac{\frac{1}{2}(|t|^{2H}+|t+h|^{2H}-|(t+h)-t|^{2H}) - |t|^{2H}}{|t|^{2H}|h|^{2H}} \\
&= \frac{(t+h)^{2H} - t^{2H} - h^{2H}}{2(th)^H}.
\end{aligned} \tag{4.5}$$

Below we will see different behavior of correlations for different values of H.

Proposition 4.2 (Independent Increments at $H = 1/2$) *If $H = 1/2$, the process is in fact Brownian motion and its increments are independent.*

Proof: From Proposition 3.3 this is readily true. Further, plugging $H = 1/2$ into Equation (4.5) gives

$$\mathbb{C}orr(B_{1/2}(t), B_{1/2}(t+h) - B_H(t)) = \frac{t+h-t-h}{\sqrt{2(th)^{1/2}}} = 0. \tag{4.6}$$

As a result, the increments are independent and our result from Browninan motion is confirmed. □

Proposition 4.3 (Correlated Increments at $H \neq 1/2$) *The following holds when $H \neq 1/2$:*

- *If $H > 1/2$ then the increments of fBm are positively correlated.*
- *If $H < 1/2$ then the increments of fBm are negatively correlated.*

Proof: Let us first define that: for $x \geq 0$,

$$g(x) = x^{2H}.$$

From the fact that

- When $H > 1/2$, let us assume $t \geq h$, then by the mean value theorem there is $u \in (t, t+h)$ such that

$$g(t+h) - g(t) = (t+h)^{2H} - t^{2H} = (2H)u^{2H-1}h > 2 \times (1/2)h^{2H-1}h = h^{2H}.$$

As a result,

$$(t+h)^{2H} - t^{2H} - h^{2H} > 0.$$

- When $H < 1/2$, the inequality

$$(a+b)^{2H} \leq a^{2H} + b^{2H}$$

holds for all $a, b \geq 0$. As a result,

$$(t+h)^{2H} - t^{2H} - h^{2H} < 0.$$

Proposition 4.3 then follows from (4.5) and the above discussion. □

4.2 Some Key Properties of Fractional Brownian Motion

One of the most important properties of fBm is the self-similarity. We say $\{B_H(t)\}_{t\geq 0}$ is H-self similar, noting that H is also called the self similarity index of the process. The self-similarity property of fBm is due to the fact that the covariance function is homogeneous of order $2H$ and can be considered as a fractal geometry property.

Proposition 4.4 (Self-similarity of fBm) *The fBm $\{B_H(t)\}_{t\geq 0}$ is H-self-similar: for any $a > 0$,*

$$\{B_H(at)\}_{t\geq 0} \sim \{|a|^H B_H(t)\}_{t\geq 0}. \tag{4.7}$$

Proof: It is easy to see both $\{B_H(at)\}$ and $\{|a|^H B_H(t)\}$ are Gaussian processes. Using the definition of Gassian process, it suffices to show $\{B_H(at)\}_{t\geq 0}$ and $\{|a|^H B_H(t)\}_{t\geq 0}$ have equal mean and covariance function.

1. Show $B_H(at)$ and $|a|^H B_H(t)$, $t \geq 0$ have equal mean. By the definition of fBm, we can write

$$\mathbb{E}\left[B_H(at)\right] = 0$$

and further by the linearity of expectation,

$$\mathbb{E}\left[|a|^H B_H(t)\right] = |a|^H \mathbb{E}[B_H(t)] = 0.$$

Therefore both $\{B_H(at)\}_{t\geq 0}$ and $\{|a|^H B_H(t)\}_{t\geq 0}$ are centered.

2. Show the covariances of the two stochastic processes $\{B_H(at)\}_{t\geq 0}$ and $\{|a|^H B_H(t)\}_{t\geq 0}$ are identical.

One one hand, using (4.1), The covariance function of $\{B_H(at)\}_{t\geq 0}$ is given by: for $0 \leq s \leq t$,

$$\begin{aligned}
&\mathbb{C}ov\left(B_H(as), B_H(at)\right) = \frac{1}{2}(|as|^{2H} + |at|^{2H} - |as - at|^{2H}) \\
&= \frac{|a|^{2H}}{2}(|s|^{2H} + |t|^{2H} - |s-t|^{2H}) = |a|^{2H}\mathbb{C}ov\left(B_H(s), B_H(t)\right).
\end{aligned} \tag{4.8}$$

One the other hand, the covariance function of $\{|a|^H B_H(t)\}_{t\geq 0}$ is given by: for $0 \leq s \leq t$,

$$\mathbb{C}ov\left(|a|^H B_H(s), |a|^H B_H(t)\right) = |a|^{2H}\mathbb{C}ov\left(B_H(s), B_H(t)\right). \tag{4.9}$$

From Equations (4.8) and (4.9) we see the covariance functions of the two processes are identical.

The proof of Proposition 4.4 is complete and we have shown that the fBm is self-similar with self similarity index H. □

Similar to Bm, fBm also has stationary increments. However its increments are not independent when $H \neq 1/2$. The stationarity of the fBm's increments can be obtained as in the following proposition.

Proposition 4.5 (Stationary increments) *The fBm $\{B_H(t)\}_{t\geq 0}$ with Hurst index $H \in (0,1)$ has stationary increments: for any $0 \leq s \leq t$,*

$$B_H(t) - B_H(s) \ \sim \ B_H(t-s). \tag{4.10}$$

Proof: The fact that $\{B_H(t)\}_{t\geq 0}$ is a centered Gaussian process yields that both $B_H(t) - B_H(s)$ and $B_H(t-s)$ are centered and normally distributed. Therefore to show (4.10) holds it remains to prove that $B_H(t) - B_H(s)$ and $B_H(t-s)$ are equal in variance. One one hand, by using the fact that for any two random variables X, Y,

$$\mathbb{V}ar(X-Y) = \mathbb{V}ar(X) + \mathbb{V}ar(Y) - 2\mathbb{C}ov(X,Y)$$

and the covariance function of fBm (4.1) we obtain the variance of $B_H(t) - B_H(s)$ as:

$$\begin{aligned} \mathbb{V}ar\left(B_H(t) - B_H(s)\right) &= \mathbb{V}ar(B_H(t)) + \mathbb{V}ar(B_H(s)) - 2\mathbb{C}ov\left(B_H(t), B_H(s)\right) \\ &= |t|^{2H} + |s|^{2H} - 2 \times \frac{1}{2}(|t|^{2H} + |s|^{2H} - |t-s|^{2H}) \\ &= |t-s|^{2H}. \end{aligned} \tag{4.11}$$

On the other hand, the variance of $B_H(t-s)$ is given by:

$$\mathbb{V}ar\left(B_H(t-s)\right) = |t-s|^{2H}. \tag{4.12}$$

It follows from Equations (4.11) and (4.12) that Proposition 4.5 holds. □

The proposition below is one of the key features of fBm. It reveals the long-range dependence of the process. This property has a number of applications in modeling the financial assets behavior. Indeed in the study of financial indices, a number of theories have recently been developed based on the assumption that the stock prices exhibit the long-range dependence. In other words the dependency between the historical and current asset prices decrease slowly. It is shown that the classical Black-Scholes model, which is driven by a standard Brownian motion, is unable to capture this feature. However if the Brownian motion is replaced by a fractional Brownian motion with Hurst index $H > 1/2$, the new Black-Scholes model displays the long-range dependence. Hence fBm plays a key role to describe the real financial market.

Proposition 4.6 (Long-range dependence of fBm.) *For $H > 1/2$ the fBm $\{B_H(t)\}_{t\geq 0}$ exhibits long-range dependence:*

$$\sum_{n=1}^{\infty} \mathbb{E}\left[B_H(1)\left(B_H(n+1) - B_H(n)\right)\right] = +\infty. \tag{4.13}$$

Heuristically speaking, (4.13) tells that the fBm's increments are dependent even as time approaches infinity. This property is also known as long-term memory. *Proof:* First by using the linearity of expectation and the covariance structure of the fBm (4.1) we can write

$$\begin{aligned} &\mathbb{E}\left[B_H(1)\left(B_H(n+1) - B_H(n)\right)\right] \\ &= \mathbb{E}[B_H(1)B_H(n+1)] - \mathbb{E}[B_H(1)B_H(n)] \\ &= \frac{1}{2}\left(|n+1|^{2H} + |1|^{2H} - |(n+1)-1|^{2H}\right) - \frac{1}{2}\left(|n|^{2H} + |1|^{2H} - |(n)-1|^{2H}\right) \\ &= \frac{1}{2}\left\{\left(|n+1|^{2H} - |n|^{2H}\right) - \left(|n|^{2H} - |n-1|^{2H}\right)\right\}. \end{aligned} \tag{4.14}$$

Observe that the main part of the right-hand side of (4.14) is in fact a second order increment of the following differentiable function:

$$f(x) = (x+1)^{2H} - x^{2H} \text{ for } x \geq 1. \tag{4.15}$$

Recall that the mean value theorem states: let g be continuous over $[a, b]$ and differentiable over (a, b), then there exists $m \in (a, b)$ such that

$$g(b) - g(a) = (b-a)g'(m). \tag{4.16}$$

By the mean value theorem (4.16), we transform Equation (4.14) to

$$\begin{aligned} &\mathbb{E}\left[B_H(1)\left(B_H(n+1) - B_H(n)\right)\right] = \frac{1}{2}\left\{f(n) - f(n-1)\right\} \\ &= \frac{1}{2}(n-(n-1))f'(m_1) = H\left\{(m_1+1)^{2H-1} - m_1^{2H-1}\right\}, \end{aligned} \tag{4.17}$$

where m_1 is some value in $(n-1, n)$. Now let us define

$$h(x) = x^{2H-1}, \text{ for } x \geq 0. \tag{4.18}$$

Since $2H-1 > 0$, the function h is continuous over $[m_1, m_1+1]$ and differentiable over (m_1, m_1+1). Therefore by the mean value theorem (4.16), (4.17) further becomes

$$\begin{aligned} &\mathbb{E}\left[B_H(1)\left(B_H(n+1) - B_H(n)\right)\right] = H\left(h(m_1+1) - h(m_1)\right) \\ &= H((m_1+1) - m_1)h'(m_2) = H(2H-1)m_2^{2H-2}, \end{aligned} \tag{4.19}$$

where m_2 is some value in $(m_1, m_1+1) \subset (n-1, n+1)$. (4.19) together with teh fact that $n-1 < m_2 < n+1$ leads to

$$H(2H-1)(n+1)^{2H-2} \leq \mathbb{E}\left[B_H(1)\left(B_H(n+1) - B_H(n)\right)\right] \leq H(2H-1)(n-1)^{2H-2}. \tag{4.20}$$

It follows from (4.20) that

$$\sum_{n=1}^{\infty} \mathbb{E}[B_H(1)\left(B_H(n+1) - B_H(n)\right)] \geq H(2H-1)\sum_{n=1}^{\infty}(n+1)^{2H-2}. \tag{4.21}$$

The fact that $H > 1/2$ implies

$$\sum_{n=1}^{\infty}(n+1)^{2H-2} \geq \sum_{n=1}^{\infty}(n+1)^{-1} = +\infty,$$

thanks to the Riemann series theorem. (4.21) then yields

$$\sum_{n=1}^{\infty} \mathbb{E}[B_H(1)\left(B_H(n+1) - B_H(n)\right)] = +\infty.$$

Proposition 4.6 is proved. □

Next we aim at discussing of some limitations of fractional Brownian motion and explaining the motivation to extend it to more general models.

Similar to Brownian motion, sample paths of fBm are continuous but almost nowhere differentiable. However, almost all trajectories are locally Hölder continuous of any order strictly less than H: for each such trajectory, for every $T > 0$ and for every $\epsilon > 0$ there exists a random constant c such that

$$|B_H(t) - B_H(s)| \approx c|t-s|^{H-\varepsilon} \tag{4.22}$$

for $0 < s, t < T$ and for arbitrarily small ε. From this formula we can see that the sample paths of B_H are hölderian functions with Hölder exponent H. The limitation of using fBm then lies on the fact that this Hölder exponent is uniform: it does not change via time. However in the real world, observed dataset often exhibits local Hölder regularity which changes with time. FBm, with constant Hölder regularity, then fails to capture this phenomena. Therefore it is required to introduce a more sophisticated process, whose local Hölder exponent is able to change with time. A natural way of extension is based on the Harmonizable representation of fBm [6, 5]:

$$B_H(t) = \int_{\mathbb{R}} \frac{e^{it\xi} - 1}{|\xi|^{H+1/2}} \, \mathrm{d}\widetilde{W}(\xi). \tag{4.23}$$

Inspired by (4.23), Benassi et al. [6] defined the multifractional Brownian motion through replacing the constant Hurst parameter H in (4.23) with a continuous function $H(t)$. The latter exponent is then called the functional Hurst parameter and the obtained process

$$X(t) = \int_{\mathbb{R}} \frac{e^{it\xi} - 1}{|\xi|^{H(t)+1/2}} \, \mathrm{d}\widetilde{W}(\xi)$$

is the so-called multifractional Brownian motion. The next section is devoted to a detailed investigation of multifractional Brownian motion.

5 From Fractional Brownian Motion to Multifractional Brownian Motion

As discussed in the previous section, the fact that the Hurst parameter H does not depend on time in fBm is sometimes undesirable as it restricts the field of application. Some phenomena do not admit a constant Holder exponent: for instance, the use of fBm for synthesizing artificial mountains does not allow to take into differing account erosion phenomena. The variation of the regularity may even contain an essential part of the signal information, unattainable with a constant H. For instance the variation of the Holder exponent has been used for images segmentation [31]. Bianchi [12] showed that H of the stock market fluctuates with market conditions, in normal markets $H > 1/2$ and during times of crisis $H < 1/2$.

An extension of the fBm, called the multifractional Brownian motion (mBm), has been proposed independently by Lévy Vehel and Peltier [21] and by Benassi, Jaffard and Roux [5]. The mBm can be defined by Definition 1.1, except that the parameter H, is replaced by a Hölder function $H(t)$, with values in $[0, 1]$. This process shares many propreties with the fBm; for instance, at any point t_0, the Hölder exponent of the mBm is, almost surely, equal to $H(t_0)$ and the mBm is asymptotically locally self-similar of order $H(t_0)$. In addition, the property of long range dependence fluctuates with the function $H(t)$, existing when $H(t) > 1/2$.

Being a natural extension of Brownian motion (Bm) and fractional Brownian motion, multifractional Brownian motion (mBm) has nowadays been successfully applied to many fields such as finance, network traffic, biology, geology and signal processing, etc. Unlike Bm and fBm, mBm is a continuous-time Gaussian process whose increment processes are generally not stationary. However, the feature that multifractional process allows its local Hölder regularity to change via time makes the process flexible enough to model a much larger class of empirical data than the fBm does.

However in the real world, the observations are often functions of multifractional Brownian motion. For example, the real world asset prices are proved to be non-Gaussian process, however their log-returns are closer to being a Brownian motion. Hence, studying the behavior of functions of multifractional Brownion motions bring interests in our research.

Multifractional processes, in particular mBm, have come into more study recently and are being widely applied to financial modeling under empirical market conditions. For example,the global financial crisis of 2008 brought strong questions about the legitimacy of the classic dichotomy between efficient and inefficient markets. It is believed that the real financial markets are too complex a

system that Bm and fBm prove too reductive to explain the entire system [12]. Unlike fBm, mBm is flexible enough to overcome this inconvenience, mainly because its PHE can vary via time as market conditions vary. Through an empirical study by Bianchi et al. [12], it was shown that the real-world stock prices can be modeled based on an mBm. Later, by estimating the PHE of the stock price dynamics, Bianchi et al. [11] finds that the PHE fluctuates around 1/2 (the sole value consistent with the absence of arbitrage), with significant deviations due to market conditions. In 2012, Bertrand et al. [7] introduces sparse modeling for mBm and apply it to NASDAQ time series data. Recently, Bianchi et al. [9] have suggested a new way to quantify how far from efficiency a market is at any fixed time t. Their dynamic approach, based on the estimation of the time-varying PHE of the log-variations of the 3 stock indexes - Dow Jones Industrial Average (DJIA), the Dax (GDAXI) and the Nikkei 225 (N225), allow them to detect the periods in which the market itself is efficient, once a confidence interval is fixed. Note that it is more difficult to estimate the PHE for mBm than it is for fBm, due to the non-stationarity of the mBm's increment processes. This problem becomes even more challenging when modeling an *individual* stock price (e.g. stock price of a particular entity) in lieu of averaged equity indexes, because the former one is not necessarily non-arbitrage and its corresponding PHE may be time-dependent and may take arbitrary values between 0 and 1 due to jumps in the stocks price. Consumer spending data is aggregated, and therefore much less likely to exhibit the same behavior as individual stocks. In this thesis one aims to provide suitable models to describe the Consumer Confidence Index (CCI) in the markets based on consumer spending (see the forthcoming Section 6).

5.1 A General Class of Multifractional Processes

Before introducing the general multifractional model that we are interested in, we briefly review the estimation of the multifractional process' PHE.

In the multifractional process modeling problem, there is an obstacle : the PHE is basically not straightforwardly observed. The issue of estimating the PHE effectively arises. There are so far a number of estimation strategies existing in literature. We refer to [15, 16, 8, 3, 18, 29] and the references therein.

Coeurjolly [15, 16] estimates the PHE of an mBm, starting from an observed discrete sample path of that mBm, using the LGQV approach (see also [14]). Bertrand et al. [8] study the same estimation problem as in [15, 16], using the nonparametric estimation approach - increment ratio (IR) statistic method. This IR estimator has been later improved by Bardet and Surgailis [3] to the so-called pseudo-increment ratio approach, and it is applied to estimate the PHE of a more general multifractional Gaussian process (whose increments are asymptotically a multiple of an fBm) than mBm. There exist other approaches to estimate the PHE of fBm, that can be possibly extended to estimate the PHE of mBm. For example, in chaos theory and time series analysis, the statistical self-affinity is another measurement of the process path roughness. Since this exponent is tightly related to the PHE of self-similar processes (e.g. fBm), the detrended fluctuation analysis (DFA) methods developed by Peng et al. [22, 23] can be used to estimate the PHE of fBm. The time-varying PHE of mBm can be then approximated by applying the DFA piecewisely over time. However, the statistical self-affinity is not equivalent to the PHE of a process, because it does not share all the properties of the Hausdorff dimension [22, 23], while the Hausdorff dimension is equivalent to the PHE when the corresponding process is self-similar. In literature, it has been shown that the wavelet-based method is actually more accurate than the DFA on estimation of the PHE. Muzy et al. [20] have obtained representations of turbulence data and Brownian signals via wavelet decompositions. Bardet et al. [2] have applied the wavelet coefficient methods to estimate the PHE of long-memory processes (e.g. fBm with its PHE being greater than 1/2), where some rate of convergence of the estimators are derived. Wendt et al. [32] have developed the wavelet leader based multifractal analysis for estimating 2D functions (images). Inspired by the above works, Jin et al. [18] have provided a wavelet-based estimator of the time-varying PHE of a class of multifractional processes with a fine convergence rate, when the observations are the wavelet coefficients of some unknown function of a multiple of mBm, i.e. the observed process is of the form $\Phi(\theta(t)X(t))$, with Φ and θ being unknown

C^2-functions, that is, continuous and smooth. In both [3] and [18], estimators of PHE with fine convergence rates are constructed and strategies for selecting input parameters are discussed.

Note that in the thesis we also consider a model more general than the one in [18], in that it allows Φ to be a function of both t and x, i.e. we assume the observed signal is some unknown function of time t and mBm X: $\Phi(t, X(t))$. We apply the LGQV-based approach to estimate the PHE of $\Phi(t, X(t))$, when one of its discrete paths is observed. Similar to Jin et al. [18], an estimator with fine convergence rate is constructed and appropriate parameter selection is discussed. In [29, 30] the oscillation estimation method, which could be applied to estimate the PHE of all processes with continuous paths, is discussed. The main advantages of our approaches are: (1) The model is simple and general enough for finance application. (2) Compared to the oscillation estimation method, the LGQV method has higher accuracy and it allows us to select the input parameter from a large range of values. This is because LGQV uses third order increments by default which is more independent than the first order increments in the oscillation method. We will provide a fine rate of convergence of our LGQV estimator, which will further help practitioners to determine the best input parameter values. (3) One disadvantage of the increment ratio approaches is that it is unable to estimate the PHE over the whole time interval $[0, 1]$. However, the algorithm for LGQV-based approach can estimate H pointwisely from $t = 0$ to $t = 1$. Moreover, it can be easily implemented using various programming languages such as Matlab, R, and Python, etc.

Throughout this paper we consider the following model: for $t \in [0, 1]$,

$$Z(t) = \Phi(t, X(t)), \tag{5.1}$$

where

- $\{X(t)\}_{t\geq 0}$ is an mBm defined in (1.3). Assume that its PHE H belongs to the class of functions $C^2([0, 1])$ (this means that H is second-order continuously differentiable over $[0, 1]$) and $[H_*, H^*] \subset (0, 1)$, where $H_* = \inf_{t\in[0,1]} H(t)$ and $H^* = \sup_{t\in[0,1]} H(t)$.
- Φ is supposed to be an unknown deterministic $C^2(\mathbb{R}_+ \times \mathbb{R})$-function. Also we assume that $\partial_y\Phi(x, y) \neq 0$ for almost every $(x, y) \in \mathbb{R}_+ \times \mathbb{R}\backslash\{0\}$ and there exist two constants c_1, c_2 such that $0 < c_1 \leq |\partial_y\Phi(x, y)| \leq c_2$ for almost every $(x, y) \in \mathbb{R}_+ \times \mathbb{R}\backslash\{0\}$.
- Suppose that a discrete sample path of Z: $\big\{Z(u/2n) : u = 0, \ldots, 2n\big\}$ is observed for some $n \in \mathbb{N}$ large enough.

From (5.1) we see that the model $\{Z(t)\}_t$ is driven only by the time index t and the mBm $\{X(t)\}_t$. It is quite general because the function Φ "lives" in a large class of functions $C^2([0, 1])$, and more importantly, it is supposed to be unknown. Examples of $\{Z(t)\}_t$ include the mBm, the self-regulating processes based on mBm [4].

5.2 LGQV Estimation of the Pointwise Hölder Exponent

Observing the discrete sample path of $Z(t) = \Phi(t, X(t))$:

$$\Big\{Z(0),\, Z\Big(\frac{1}{2n}\Big),\, Z\Big(\frac{2}{2n}\Big), \ldots,\, Z\Big(\frac{2n-1}{2n}\Big),\, Z(1)\Big\},$$

where n denotes an integer large enough, our goal is to propose a method allowing to estimate the PHE $H(t_0)$ of the hidden mBm $\{X(t)\}_{t\in[0,1]}$ at an arbitrary time $t_0 \in (0, 1)$. To this end, we apply a localized generalized quadratic variations (LGQV) estimation method. Before stating our main results, we need to briefly introduce some notations which will be used throughout the rest of the paper.

- As usual, $a = (a_0, \ldots, a_p) \in \mathbb{R}^{p+1}$ is an arbitrary but fixed finite sequence having $Q \geq 1$ vanishing moments, that is,

$$\sum_{k=0}^{p} k^l a_k = 0, \text{for } l = 0, \ldots, Q-1 \text{ and } \sum_{k=0}^{p} k^Q a_k \neq 0. \tag{5.2}$$

This shows the reader that our estimator will converge within reasonable timing.

- For all integer $n \geq p+1$ and $i \in \{0, \ldots, n-p-1\}$ the generalized increments of Z, $\Delta_a Z_{i,n}$, and that of X, $\Delta_a X_{i,n}$, are defined by,

$$\Delta_a Z_{i,n} := \sum_{k=0}^{p} a_k Z_{i+k,n} \text{ and } \Delta_a X_{i,n} := \sum_{k=0}^{p} a_k X_{i+k,n}, \tag{5.3}$$

where $Z_{i+k,n}$ and $X_{i+k,n}$ denote the values of the processes Z and X, at time $(i+k)/n$, that is,

$$Z_{i+k,n} := Z\Big(\frac{i+k}{n}\Big) \text{ and } X_{i+k,n} := X\Big(\frac{i+k}{n}\Big). \tag{5.4}$$

- For all integer $n \geq p+1$, we denote by $\nu_n(t_0)$ the set of indexes defined by,

$$\nu_n(t_0) = \Big\{ i \in \{0, \ldots, n-p-1\} : \ \Big|\frac{i}{n} - t_0\Big| \leq v(n) \Big\}, \tag{5.5}$$

where $v(\cdot)$ is an arbitrary function of $n \geq p+1$, valued in $(0,1]$, which satisfies for each integer $n \geq p+1$, $v(n) \geq n^{-1}$ and $\lim_{n\to\infty} nv(n) = \infty$. Note that $\nu_n(t_0)$ labels the times t in the neighborhood of t_0. As mentioned in [15, 16], the estimation of $H(t_0)$ only relies on the observations of $Z(t)$, for t being "neighbored to" t_0. Consequently, the estimation accuracy will be in terms of the size of the neighborhood selected for each t_0. Both theoretical and empirical studies tend to show that, the size of the neighborhood shouldn't be chosen too large nor too small, i.e. there is a trade-off between the estimator's rate of convergence and bias.

- For all integer $n \geq p+1$ we define n_{t_0} to be the number of points in $\nu_n(t_0)$:

$$n_{t_0} = \#\nu_n(t_0). \tag{5.6}$$

We then quickly observe that

$$n_{t_0} \in \big\{ [2nv(n)], [2nv(n)]+1 \big\}, \tag{5.7}$$

where $[\cdot]$ is the integer part function.

Now we are ready to construct a LGQV consistent estimator of $H(t_0)$, $t_0 \in [0,1]$ of $\{Z(t)\}_{t\in[0,1]}$. Recall that, in statistics theory, an estimator $\hat{\theta}_n$ of a parameter θ is (weakly) consistent if $\hat{\theta}_n$ converges to θ in probability, as $n \to \infty$. Let $\{U_n\}_{n\geq 1}$ be an arbitrary sequence of random variables and $\{v_n\}_{n\geq 1}$ be a sequence of non-vanishing real numbers, we use the notations

$$U_n = \mathcal{O}_{a.s.}(v_n) \text{ and } U_n = \mathcal{O}_{\mathbb{P}}(v_n)$$

to denote

$$\mathbb{P}\left(\sup_{n\geq 1} \frac{|U_n|}{|v_n|} < \infty\right) = 1 \text{ and } \lim_{\eta\to\infty} \sup_{n\geq 1} \mathbb{P}\left(\frac{|U_n|}{|v_n|} > \eta\right) = 0, \text{ respectively.}$$

Remark that $U_n = \mathcal{O}_{a.s.}(v_n)$ leads to $U_n = \mathcal{O}_{\mathbb{P}}(v_n)$, and the almost sure convergence implies the convergence in probability.

Our first main result below provides a delicate identification of the covariance of the generalized increments of the multifractional process of a particular form $Y(t) = \sigma(t)X(t)$. Later we will need this result for estimating the PHE of the more general function of $X(t)$: $Z(t) = \Phi(t, X(t))$.

Proposition 5.1 *Let $\{X(t)\}_{t\in[0,1]}$ be an mBm and $Y(t) = \sigma(t)X(t)$, with σ being a second order stochastic process independent of X, and the bivariate function $\theta(s,t) := \mathbb{E}(\sigma(s)\sigma(t))$ satisfies $\theta \in C^2([0,1]^2)$. For a sequence $a \in \mathbb{R}^{p+1}$, assume $Q \geq 2$, then for every $k, k' \in \{0, 1, \ldots, n-p-1\}$, we have,*

(1) *if* $k \neq k'$,

$$Cov(\Delta_a Y_{k,n}, \Delta_a Y_{k',n}) = C\left(H(\frac{k}{n}) + H(\frac{k'}{n}), Q\right)\left(\frac{n^{-H(k/n)-H(k'/n)}\theta(k/n, k'/n)}{|k-k'|^{2Q-H(k/n)-H(k'/n)}}\right) + n^{-H(k/n)-H(k'/n)}R(n,k,k',Q), \tag{5.8}$$

where

- $C \in C^2([0,1]\times\mathbb{R}_+)$ *is some deterministic function.*
- *The remaining term* $R(n,k,k',Q)$ *satisfies*

$$\sum_{0\leq k,k'\leq n} |R(n,k,k',Q)|^2 = \mathcal{O}\left(n^{-1}(\log(n))^2\right).$$

(2) *The variance of* $\Delta_a Y_{k,n}$ *can be identified as below:*

$$Var(\Delta_a Y_{k,n}) = C_1(\frac{k}{n})n^{-2H(k/n)} + \mathcal{O}(n^{-2H(k/n)-1}|\log n|^4), \tag{5.9}$$

where the coefficient $C_1(k/n)$ *is a deterministic constant.*

We quickly point out that, in the above proposition, there is not any inconvenience to regard σ to be a $C^2([0,1])$ class deterministic function. It is also worth noting that Proposition 5.1 has its own interests, since it gives an exact estimation of the covariance structure of the generalized increments of $Y(t) = \sigma(t)X(t)$, with a fine rate of convergence for its remaining term. To motivate the above facts we briefly compare Proposition 5.1 to Lemma 1 in [15] below:

1. Proposition 5.1 extends Lemma 1 in [15] from mBm $X(t)$ to a stochastic volatility process $Y(t) = \sigma(t)X(t)$, which is a useful model in financial time series analysis.
2. Unlike (iii) in Lemma 1 in [15], Proposition 5.1 provides a finer identification of $\pi_H^a(k)$, by discovering a fine identification of the remaining term.
3. The only difference of assumptions on H between Proposition 5.1 and Lemma 1 in [15] is that we assume $H \in C^2([0,1])$, while in [15] it is assumed that $H \in C^\eta([0,1])$ with $\eta \in (0,1)$.

The proof of Proposition 5.1 can be found in [26]. The motivation of Proposition 5.1 is bi-fold:

(1) As a simple case, it indicates that: for $s < t$ and $|t-s|$ sufficiently small,

$$|X(t) - X(s)| \approx |t-s|^{H(t)-\varepsilon}, \tag{5.10}$$

for any $\varepsilon > 0$ arbitrarily small. The approximation equation (5.10) accurately explains the role that $H(t)$ plays: it explains the "volume" of the jump of X from time s to t. In other words the PHE $H(\bullet)$ measures the local variance of the increments (or volatility) of the multifractional Brownian motion X. Comparing H among different mBms' paths are equivalently comparing volatilities of mBms. These provide a new way to perform factor analysis: study the factor impact on the PHE, instead of the factor impact on the value of the process. In short, in this new idea, the factor importance is based on the volatility, not the trend of the process.

(2) Proposition 5.1 leads to the LGQV estimator of the PHE of the multofractional process Z, see Theorem 5.2 below.

The second main result involves estimation of the PHE of the general process $Z(t) = \Phi(t, X(t))$, under a very general condition:

Theorem 5.2 *Pick a sequence* $a \in \mathbb{R}^{p+1}$ *with its first* $Q \geq 2$ *moments being vanishing. We list the following conditions on* $v(n)$.

(i) $v(n)$ satisfies:

$$\lim_{n\to\infty} \sum_{l=0}^{4} v(n)^l n^{(l-2)H(t_0)} |\log n|^{2-l/2} = 0, \text{ for all } t_0 \in (0,1).$$

(ii) $v(n)$ satisfies:

$$\sum_{n\geq p+1} \frac{1}{(nv(n))^2} < \infty.$$

For $t_0 \in (0,1)$, define

$$V_n(t_0) = \sum_{i\in\nu_n(t_0)} \left(\Delta_a Z_{i,n}\right)^2, \tag{5.11}$$

and

$$\widehat{H}_{n,t_0} = \frac{1}{2}\left(1 + \log_2\left(\frac{v(2n)}{v(n)}\right) + \log_2\left(\frac{V_n(t_0)}{V_{2n}(t_0)}\right)\right), \tag{5.12}$$

where $\log_2$ is the base-2 logarithm.
***(1)** If $v(n)$ satisfies the condition (i), we have*

$$\begin{aligned}
&\widehat{H}_{n,t_0} - H(t_0) \\
&= \mathcal{O}_{a.s.}\left(\left(\sum_{l=0}^{4} v(n)^l n^{(l-2)H(t_0)} |\log n|^{2-l/2}\right)^{1/2} + v(n)^{H(t_0)} |\log(v(n))|^{1/2}\right) \\
&\quad + \mathcal{O}_{\mathbb{P}}\left(v(n)\log n + v(n)^{-1} n^{-1}\right).
\end{aligned}$$

***(2)** If $v(n)$ satisfies the conditions (i)-(ii), then*

$$\widehat{H}_{n,t_0} \xrightarrow[n\to\infty]{a.s.} H(t_0),$$

where $\xrightarrow[n\to\infty]{a.s.}$ denotes the convergence almost surely.

Theorem 5.2 is our key result. It provides consistent estimators of the PHE of $\{Z(t)\}_t$ in a very general setting. Moreover, Theorem 5.2 (1) elaborates the rate of convergence of the estimators. We see that the rate of convergence depends only on the sample size n and $v(n)$. The proof of Theorem 5.2 is provided in [26].

6 Real World Application: Factor Analysis on Consumer Confidence Index

In order to motivate the multifractional processes modeling that we have introduced in the previous sections, we take a real world application: we attempt to study the importances of factors which explain the behavior of the Consumer Confidence Index (CCI) from consumer spending data. CCI provides an overview of the average spenders outlook towards the market at large from widely collected survey data in the United States. It represents the optimism or pessimism that consumers are likely to spend with in the next six months. This index can be explained jointly by a number of factors from both social economics and finance and individual spending and investing behavior. Therefore CCI is used across industries including banks, investors, manufacturers, and other businesses to predict how the market will do. Consumers will spend more on luxury goods and pay higher prices for investment goods. On the contrary a low CCI can indicate a potential drop in stocks or spending. Since CCI can have an impact on the stock market and the decision making processes of different businesses, predicting how it will change is valuable. Despite the widespread power of

surveying of consumer confidence, the mechanisms by which household consumption behavior influences household attitudes are less well understood. Consumer opinion surveys ask respondents about their household purchases because their present financial situation is a crucial component in calculating CCI. However, the household cannot be completely sure of their future spending habits because finances can be uncertain, so a more robust predictor could be valuable . To predict the value of CCI we will apply the mBm model to a number of factors and compare them to the mBm model of CCI. These factors are actual spending data for different sectors of the economy summed up for the same time period of the CCI reporting. Since CCI is survey data and the factors are spending data there is no risk of collinearity between the two.

Using two sets of monthly time-series datasets, we estimate the mutual relationship between consumer attitudes measured by the consumer confidence index (CCI) and the household consumption expenditures. One set is the CCI which is published by the Organisation for Economic Co-operation and Development (OECD) for 2002 through 2020. The CCI is calculated as a simple average of survey responses based on respondents' past and expected financial and economic situation. This sentiment indicator provides an indication of future developments of households' consumption and saving. When the CCI value above 100 indicates an optimistic attitude toward future economic developments, possibly lead individuals in spending more money in the next 12 months. In comparison, values below 100 signal a decrease in consumers' confidence toward the future economic situation, as a result of which individuals save more and spend less. We also encompass eleven household consumption expenditures in the datasets such as education and recreation spending. This information is provided by the Bureau of Economic Analysis (BEA) of the United States Department of Commerce, a U.S. government agency that provides official macroeconomic statistics. Overall, we conduct 228 months of the CCI and household consumption expenditures together to evaluate who drives consumers confidence.

The specific sectors of the market we will use to predict CCI and the details on the features of the variables are outlined in Table 1.

Response	Factor
CCI	Food
	Clothing
	Housing
	Household expenses
	Health
	Transportation
	Communication
	Recreation
	Education
	Financial services

Table 1: Householder expenditure variables in Dataset

Using the technique developed in the previous section, the pointwise Hölder exponent was estimated for both CCI and the consumer expenditure variables. Assuming each time series is a continuous-time multifractional process described as in (5.1), we display their corresponding OSC and LGQV estimators of pointwise Hölder exponents and compare a Euclidean and correlations mixture distance among these estimators. Figure **??** below illustrates the PHEs of each paths of CCI and household expenditures in Table 1.

In both estimation methods, we force the estimated values of PHEs to be 0 or 1 if they are negative or greater than 1, because these issues are due to the lack of estimation accuracy. From Figure **??** we see the 2 estimators have quite different outcomes. This may be explained as: the

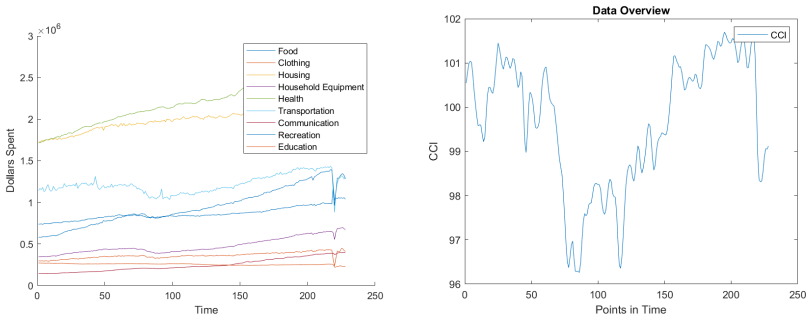

Figure 1: Graphs of the sample data of Categorical Spending Data and CCI Values.

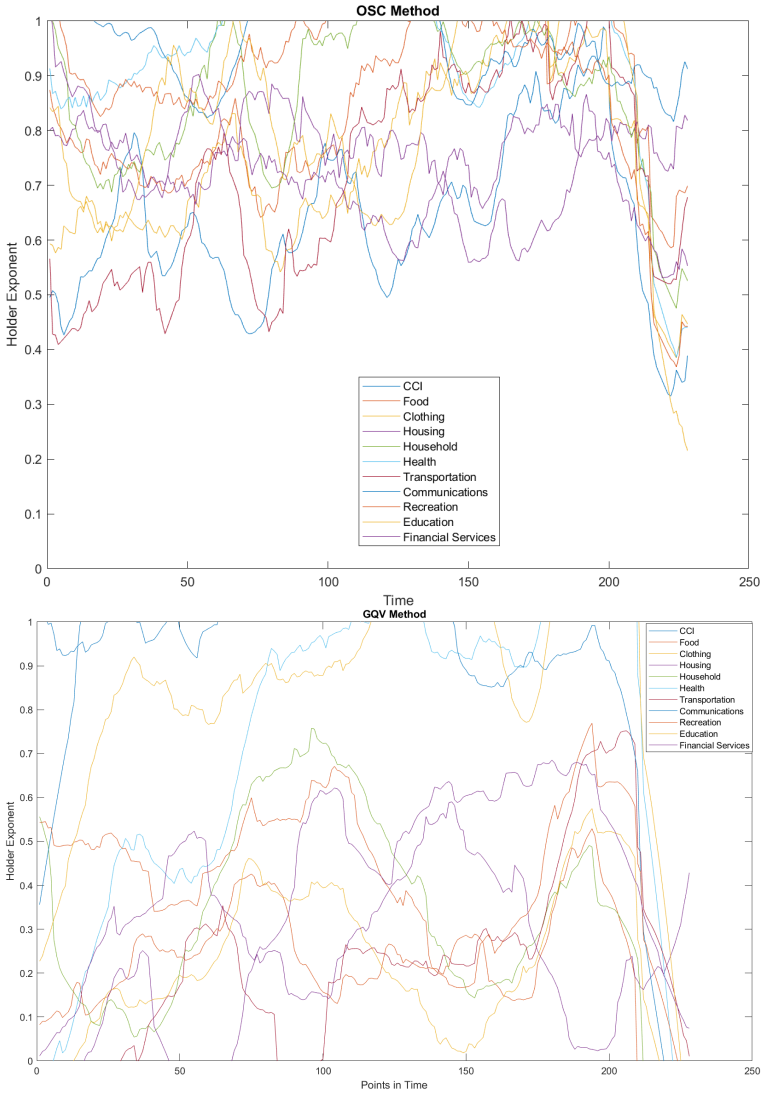

Figure 2: Comparison of PHEs by OSC and LGQV Estimation Methods

OSC method converges not fast enough [29, 30][1]. Therefore our next step analysis will rely more on

[1]OSC represents the first order increments case of LGQV.

the results from the LGQV method.

From Figure 2 we see the PHE of the data from 2002 to 2020. In 2008 (around point 100) there is a barely noticeable change in the PHE, but due to COVID-19 in 2020 (after point 220) PHE drops as the correlation gets negative and the data gets more rough. COVID-19 had a huge effect on both the lively hood and mental health of many consumers in the US, explaining this drop.

Next we perform cluster analysis to detect household expenditure factors which have similar patterns to the CCI. To this end we run K-means clustering to cluster all the estimated PHEs output by the 2 estimators. It is worth noting that, in this clustering we define the dissimilarity function to be a mixture of Euclidean distance and the covariance matrix distance. This is because, we wish the similarity of 2 PHEs are presented in terms of both mean and variance.

The clustering results (based on the PHEs estimated by the LGQV method) are given in Table 2 below:

Variable\Number of clusters	1	2	3	4	5	6	7	8	9	10	11
CCI	0	1	1	0	1	1	0	2	2	0	10
Food	0	0	0	1	0	0	1	1	0	9	9
Clothing	0	0	0	1	0	0	1	1	0	6	6
Housing	0	0	2	2	2	5	5	5	5	5	5
Household Equipment	0	0	0	1	0	2	2	0	8	8	8
Health	0	1	1	0	4	4	4	4	4	4	4
Transportation	0	0	0	1	0	0	6	6	6	2	2
Communication	0	1	1	0	1	1	0	2	2	0	7
Recreation	0	0	0	1	0	2	2	0	7	7	3
Education	0	1	1	0	1	1	0	7	3	3	1
Financial Services	0	0	0	3	3	3	3	3	1	1	0

Table 2: Cluster Labels of PHEs from the LGQV Method. Variables with equal cluster label are grouped. The clusters are obtained by using K-means method with $K = 1, \ldots, 11$.

For K-means clustering, the Factors are grouped into consecutively more groups as the factor analysis is run with every factor in the same group to start and in their own group to finish. As the number of groups expand and group size gets smaller, two factors being in the same group has increased importance. CCI and Communication share the 10th cluster,and every group before that, making Communication Spending the most important factor in the prediction of the movement of CCI. The $H(t)$ functions are the most similar between communication and CCI, revealing their variances are most similar. The effect of $H(t)$ on variance is a result of the LGQV Estimator and is further demonstrated in Equation 7.1 which we will examine later.

A number of other factors have an similarity to that of CCI. In the 7th cluster, Education Spending in in the same group as CCI making it the second most important factor. Health Spending is the final factor importance with CCI, and no other Factor is clustered with CCI. The rankings are available to view in Table 3.

Ranking	Factor
1	Communication
2	Education
3	Health

Table 3: Factor importance ranking from cluster analysis. The three factors that best predict the changes in the increments are Spending on Communication, Education, then Health, in that order.

7 Model Specifics: Limitations and Future Applications

Finally we explain the rationals of ranking factors based on comparing the PHEs instead of linear regression. Below we express how the PHE $H(t)$ explains the behavior of a multifractional process:

$$\mathbb{E}[Z(t+\tau) - Z(t)]^2 \sim c^2(t)\tau^{2H(t)}, \quad \text{as } \tau \to 0. \tag{7.1}$$

In Equation 7.1 we can see more clearly the relationship between the $H(t)$ function and the variance of an increment of the process. As $H(t)$ changes, so does the variance of the function. Since the three factors have the most similar $H(t)$ functions to CCI, their movements will predict the changes in the variance of CCI.

However our analysis does encounter some limitations. First, CCI is only asking households their predictions for 6 months of future spending data predictions, so getting survey data on other time frames could be valuable. The data is also only for the United States so other countries may have different predictors or significant factors. Factors other than spending categories may be more relevant to CCI, such as unemployment data or more macroeconomic factors of GDP beyond household spending. Further the H function is limited to time series data and would not be able to pull conclusions from unordered data. The H value is local and does not take into account a large set of data for the calculation of $H(t)$. With these limitations, we still see some benefits.

Our predictor is different than a classical regression where the variance would be held constant as the predictor is solely based on the deviation from the mean. The lack of a variable variance fails to tell the whole story of the data and provide a complete prediction. Given that to have the complete definition of a distribution in statistics you need both the mean and the variance, it is necessary that future prediction models involve both the mean and variance. Including the estimation of variance is our main motivation for introducing multifractional Brownian motion, and we believe that the model will have many further applications beyond household spending data and the Consumer Confidence Index.

Back to the origins of Bm, the further applications of the mBm based model are in the biological and finance spaces. In functional Magnetic Resonance Imaging (fMRI) analysis of neural signals the variability modelling is possibly more accurate. for detecting the activity of the brain. The variance modelling could make predicting the spread of viruses, specifically COVID-19, more accurate. In finance variance modelling may have broader applications than CCI when it comes to Market Share dynamics, predicting growth, or the flow of Venture Capital and Private Equity funding. One might also view more macroeconomic trends such as innovation indicators such as patent fillings and IPO data, or downturn indicators like unemployment rates with the mBm modelling techniques.

References

[1] Antoine Ayache and Jacques Lévy-Véhel. On the identification of the pointwise Hölder exponent of the generalized multifractional Brownian motion. *Stochastic Processes and their Applications*, 111(1):119–156, 2004.

[2] J M Bardet, G Lang, E Moulines, and P Soulier. Wavelet estimator of long-range dependent processes. *Statistical Inference for Stochastic Processes*, 3(1–2):85–99, 2000.

[3] Jean-Marc Bardet and Donatas Surgailis. Nonparametric estimation of the local Hurst function of multifractional Gaussian processes. *Stochastic Processes and their Applications*, 123(3):1004–1045, 2013.

[4] Olivier Barrière, Antoine Echelard, and Jacques Lévy-Véhel. Self-regulating processes. *Electronic Journal of Probability*, 17(103):1–30, 2012.

[5] A Benassi, S Jaffard, and D Roux. Gaussian processes and pseudodifferential elliptic operators. *Rev. Mat. Iberoamericana*, 13(1):19–89, 1997.

[6] Albert Benassi, Daniel Roux, and Stéphane Jaffard. Elliptic Gaussian random processes. *Revista Matemática Iberoamericana*, 13(1):19–90, 1997.

[7] Pierre R Bertrand, Abdelkader Hamdouni, and Samia Khadhraoui. Modelling nasdaq series by sparse multifractional Brownian motion. *Methodology and Computing in Applied Probability*, 14(1):107–124, 2012.

[8] Pierre Raphaël Bertrand, Mehdi Fhima, and Arnaud Guillin. Local estimation of the Hurst index of multifractional Brownian motion by increment ratio statistic method. *ESAIM: Probability and Statistics*, 17:307–327, 2013.

[9] Sergio Bianchi and Massimiliano Frezza. Fractal stock markets: international evidence of dynamical (in) efficiency. *Chaos: An Interdisciplinary Journal of Nonlinear Science*, 27(7):071102, 2017.

[10] Sergio Bianchi, Alexandre Pantanella, and Augusto Pianese. Modeling and simulation of currency exchange rates using multifractional process with random exponent. *International Journal of Modeling and Optimization*, 2(3):309, 2012.

[11] Sergio Bianchi, Alexandre Pantanella, and Augusto Pianese. Modeling stock prices by multifractional Brownian motion: an improved estimation of the pointwise regularity. *Quantitative Finance*, 13(8):1317–1330, 2013.

[12] Sergio Bianchi and Augusto Pianese. Multifractional properties of stock indices decomposed by filtering their pointwise Hölder regularity. *International Journal of Theoretical and Applied Finance*, 11(06):567–595, 2008.

[13] Brahim Boufoussi, Marco Dozzi, and Raby Guerbaz. Path properties of a class of locally asymptotically self-similar processes. *Electronic Journal of Probability*, 13(29):898–921, 2008.

[14] Grace Chan, Peter Hall, and DS Poskitt. Periodogram-based estimators of fractal properties. *The Annals of Statistics*, pages 1684–1711, 1995.

[15] Jean-François Coeurjolly. Identification of multifractional Brownian motion. *Bernoulli*, 11(6):987–1008, 2005.

[16] Jean-François Coeurjolly. Erratum: Identification of multifractional Brownian motion. *Bernoulli*, 12(2):381–381, 2006.

[17] Sixian Jin, Qidi Peng, and Henry Schellhorn. Estimation of the pointwise Hölder exponent of hidden multifractional Brownian motion using wavelet coefficients. *Statistical Inference for Stochastic Processes*, 21(1):113–140, 2018.

[18] Sixian Jin, Qidi Peng, and Henry Schellhorn. Estimation of the pointwise Hölder exponent of hidden multifractional Brownian motion using wavelet coefficients. *Statistical Inference for Stochastic Processes*, 21(1):113–140, 2018.

[19] B Mandelbrot and J W van Ness. Fractional Brownian motions, fractional noises and applications. *SIAM Review*, 10(4):422–437, 1968.

[20] J F Muzy, E Bacry, and A Arneodo. Wavelets and multifractal formalism for singular signals: Application to turbulence data. *Phys. Rev. Lett.*, 67:3515–3518, 1991.

[21] Romain François Peltier and Jacques Lévy-Véhel. Multifractional Brownian motion: definition and preliminary results. *Rapport de recherche de l'INRIA, INRIA*, 2645:239–265, 1995.

[22] C K Peng, S V Buldyrev, S Havtin, M Simons, H E Stanley, and A L Goldbergerz. Mosaic organization of dna nucleotides. *Physical Review E*, 49(2):1685–1689, 1994.

[23] C K Peng, S Havtin, H E Stanley, and A L Goldbergerz. Quantification of scaling exponents and crossover phenomena in nonstationary heartbeat time series. *Chaos*, 5(1):82–87, 1995.

[24] Qidi Peng. Statistical inference for hidden multifractional processes in a setting of stochastic volatility models, 2011.

[25] Qidi Peng. Uniform Hölder exponent of a stationary increments Gaussian process: estimation starting from average values. *Statistics & Probability Letters*, 81(8):1326–1335, 2012.

[26] Qidi Peng and Ran Zhao. A general class of multifractional processes and stock price informativeness. *Chaos, Solitions & Fractals*, 115:248–267, 2019.

[27] A Pianese, S Bianchi, and A M Palazzo. Fast and unbiased estimator of the time-dependent Hurst exponent. *Chaos: An Interdisciplinary Journal of Nonlinear Science*, 28(3):031102, 2018.

[28] Stilian A Stoev and Murad S Taqqu. How rich is the class of multifractional Brownian motions? *Stochastic Processes and their Applications*, 116(2):200–221, 2006.

[29] Claude Tricot. *Curves and fractal dimension*. Springer Science & Business Media, 1994.

[30] Leonardo Trujillo, Pierrick Legrand, Gustavo Olague, and Jacques Lévy-Véhel. Evolving estimators of the pointwise Hölder exponent with genetic programming. *Information Sciences*, 209:61–79, 2012.

[31] Jacques Lévy Véhel. Introduction to the multifractal analysis of images, 1998.

[32] H Wendt, S G Roux, S Jaffard, and P Abry. Wavelet leaders and bootstrap for multifractal analysis of images. *Journal of Signal Processing*, 89(6):1100–1114, 2009.

[33] Norbert Wiener. Collected works, vol. 1, p. masani. 1976.